IL NUOVO CIMENTO VOL. 13 A, N. 3 1 Febbraio 1973

Resonance Production and Inclusive Cross-Sections in Dual Models.

L. MASPERI (*) and C. REBBI (**)
CERN - Geneva

(ricevuto l'1 Settembre 1972)

Summary. — We compute numerically the contribution to inclusive spectra of produced intermediate resonances through the discontinuity of one-loop dual amplitudes. We find these contributions to be smaller but not negligible as compared to those coming from tree graphs. Scaling may be reached for loop diagrams at higher energies than trees. The cut-off in transverse momentum is preserved even for rather heavy intermediate produced resonances. We argue that this fact is related with strong polarization effects in the decay of resonances in the dual model.

1. – Introduction and summary of results.

A definite contribution to inclusive cross-sections can come from the production and subsequent decay of a resonance, according to the scheme $a+b \to R+X$, $R \to c+X'$, where X and X′ are unobserved particles.

The relevance of such a mechanism for the theoretical interpretation of the inclusive cross-sections varies very much according to the model which is adopted [1]; in this article we investigate the rôle it plays in the dual-resonance model.

(*) On leave of absence from Centro Atomico Bariloche and Istituto de Fisica Balseiro (CNEA y UNC), Bariloche, Argentina.
(**) On leave of absence from Istituto di Fisica Teorica dell'Università, Trieste.
(1) E. L. BERGER: Argonne preprints ANL/HEP 7134 and 7148 (1971); E. YEN and E. L. BERGER: *Phys. Rev. Lett.*, **24**, 695 (1970); L. BRINK, W. N. COTTINGHAM and S. NUSSINOV: *Phys. Lett.*, **37** B, 192 (1971).

Resonance production can be related, via the Mueller theorem (2), to a discontinuity of a forward $3 \to 3$ amplitude, in which one of the three interacting particles is an excited state.

In the dual-resonance theory this amplitude receives contributions of increasing order in the over-all coupling constant g from the tree diagrams, the one-loop diagrams and so on.

The simplest and most likely the dominant contribution originates by the tree diagrams when they are compatible with the quantum numbers of the intervening particles. We are thus led to consider the discontinuities of tree diagrams, in which two of the external lines represent excited states. Two typical diagrams in which we shall be interested are those of Fig. 1. We have chosen them to characterize the two different situations in which resonances are present (Fig. 1 *a*)) or absent (Fig. 1 *b*)) in the initial ab channel. To compute the contribution of resonance production to inclusive cross-sections we must let the resonance decay and sum over the unobserved decay products. We must also sum over the various resonances that can be produced.

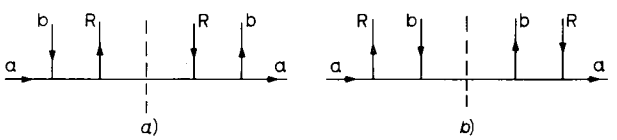

Fig. 1. – Some tree diagrams for resonance production.

A convenient way to perform the computation is to use the one-loop formula of the dual-resonance theory. We can in fact describe the production and subsequent decay of on-mass-shell resonances simply by replacing the double poles of the form $1/(k^2 - m_R^2)^2$ that appear in the integrand of the loop amplitude with a factor $\pi\delta(k^2 - m_R^2)/\Gamma_R m_R$, where k is the internal momentum of the loop and m_R and Γ_R are the masses and widths of the resonances.

Then the contributions to inclusive cross-sections associated with the production mechanism of Fig. 1 *a*) and 1 *b*) are represented by the loop diagrams of Fig. 2 *a*) and 2 *b*); it must be stressed, however, that the sum over the resonances R is performed only over those resonances that can get on the mass shell in the integration over the internal momentum, and that the corresponding product of propagators is replaced by a δ-function. The sum over unobserved final particles is performed by taking the discontinuity in the $ab\bar{c}$ channel, according to the Mueller theorem.

The factor $\pi\delta(k^2 - m_R^2)/\Gamma_R m_R$ can be considered as the narrow-width limit of the product of propagators $(1/k^2 - m_R^2 + i\Gamma_R m_R) \times (1/k^2 - m_R^2 - i\Gamma_R m_R)$, where the width of the resonances has been inserted to take account of their decay

(2) A. H. MUELLER: *Phys. Rev. D*, **2**, 2963 (1970).

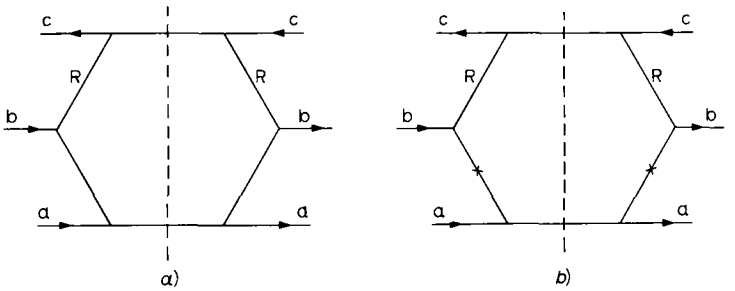

Fig. 2. – Some loop diagrams for the contribution of resonance production to inclusive cross-sections.

(the opposite signs of the terms $i\Gamma_R m_R$ derive from the opposite $i\varepsilon$ prescription in the Mueller theorem).

Notice that the width of the resonances is of order g^2 in the over-all coupling constant that characterizes the dual expansion: it follows that the contribution to inclusive cross-sections which comes from production of resonances is of the same order of magnitude in g as the direct-production term that can be computed from the discontinuity of the tree graphs ([3]).

The inclusive spectra resulting from the tree graphs of the dual model have been the object of extensive investigations ([4]).

Notice that the tree graphs do not account for the process of resonance production and subsequent decay, which we study in this article. This can be seen from the examples of Fig. 1, where we take R to be the final observed particle c: some of the tree graphs do contain resonance *formation* in the initial ab channel (Fig. 1 *a*)), but the detected particle c never comes from the decay of a *produced* resonance.

When dealing with dual models one has to be always very careful with the problem of possible double countings. In our case one may ask oneself whether the contributions that we are computing are not somehow already included in the tree graphs. The following argument might be brought up: the contribution of R to the amplitude for $a+b\to c+$two intermediate resonances (R_1R_2) might be dualized according to the scheme of Fig. 3. If this dualization is possible, the contribution to the inclusive cross-section coming from the resonances

---

([3]) A. DI GIACOMO, S. FUBINI, L. SERTORIO and G. VENEZIANO: *Phys. Lett.*, **33** B, 171 (1970); G. VENEZIANO: *Proceedings of the International Conference on Duality and Symmetry in Hadron Physics* (Tel Aviv, 1971).

([4]) D. GORDON and G. VENEZIANO: *Phys. Rev. D*, **3**, 2116 (1971); M. A. VIRASORO: *Phys. Rev. D*, **3**, 2834 (1971); C. E. DETAR, K. KANG, C. I. TAN and J. H. WEIS: *Phys. Rev. D*, **4**, 425 (1971); R. J. BIEBL, D. BEBEL and D. EBERT: Berlin-Zeuthen preprint PHE 71-9 (1971); R. C. ARNOLD and S. FENSTER: Argonne preprint ANL/HEP 7122 (1971); G. H. THOMAS: Argonne preprint ANL/HEP 7144 (1971); D. BEBEL, K. J. BIEBL, D. EBERT and H. J. OTTO: Berlin-Zeuthen preprint PHE 71-13 (1971).

R should not be added to the tree-graph term, because the diagram with the resonances R′ in Fig. 3 is in fact already contained in the tree graph (*).

This problem has been discussed at length in ref. (5). The answer is that the dualization depicted in Fig. 3 is not allowed for narrow resonances, because one is dealing with the square of an amplitude.

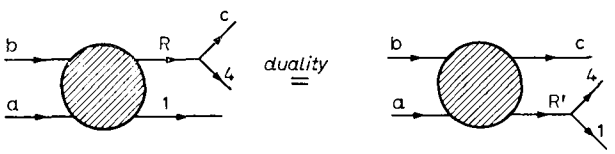

Fig. 3. – A dualization of resonance contributions discussed in the text.

The crux of the matter is whether the resonances R are in fact seen as individual bumps in the R_2-c channel or average to a continuum. In the first case the dualization is not allowed and the contributions coming from the production of resonances must be added to that of the tree graphs.

A more difficult problem is to deal with the production term where the resonances do average to a continuum, and also to analyse the transition region. In this paper we shall not examine this question but will study the contributions to inclusive cross-sections that can come from the production of narrow resonances well separated in energy, such as the first low-lying ones.

This discussion already outlines the method of computation we shall follow in the article: we will evaluate the discontinuities in the missing-mass variable of some of the loop amplitudes, with the propagators of the resonances R replaced by a δ-function. To be more specific, we shall perform numerical computer calculations of a variety of spectra of the observed particle, based on an expansion of the loop formula which we will discuss in Sect. 2. We then discuss the features, revealed by the computation, which we believe to be characteristic of the dual-resonance model.

An alternative approach would have consisted in deducing asymptotic spectra: the numerical and asymptotic methods are in this case complementary, because the numerical computation finds its limitation, due to the increasing number of channels to be taken into account, probably where an asymptotic regime begins. We have chosen to perform numerical computations because we felt these would give more accurate predictions in a range of squared centre-of-mass

(*) We acknowledge a very useful exchange of correspondence with G. VENEZIANO on this and related problems. See also the footnote (14) of the first paper in ref. (4).

(5) F. ARBAB, J. C. GALLARDO, L. MASPERI and C. REBBI: *Lett. Nuovo Cimento*, **2**, 1245 (1971); J. C. GALLARDO and L. MASPERI: *Lett. Nuovo Cimento*, **3**, 261 (1972); J. C. GALLARDO, L. MASPERI and C. REBBI: Trieste Internal Report IC/71/151 (1971).

energies ($s \simeq 6 \div 24$, in units of inverse slope of Regge trajectories $(\alpha')^{-1}$) of particular interest from an experimental point of view.

The most relevant results that we extract from the calculations, which will be discussed in Sect. **3**, are

a) The contributions to inclusive cross-sections coming from the decay of a produced resonance according to the mechanism of Fig. 2 are smaller but not negligible with respect to those coming from the direct emission represented by the tree graphs. Typically, the loop can give corrections ranging from few percent to 20% or 30% independent of the value of the coupling constant g.

b) *The cut-off in transverse momentum is preserved, even when the final particle results from the decay of a rather heavy resonance.*

c) A scaling regime may be obtained for the loop, but it starts much higher than for the tree formula.

A characteristic that we find extremely relevant is given by point *b*) above. Notice in fact that some of the produced resonances release enough kinetic energy in their decay that the spectrum of the emitted particles might be rather broad in transverse momentum even if the resonances are produced with a cut-off, unless there are strong polarization effects. Our results seem to indicate that such effects are present in the dual model.

As a check, in Sect. **4**, we shall project out of our formulae the amplitude for the production of the first excited resonance of spin 1. We evaluate the spectrum and the density matrix of spin states: the results show indeed that the resonance is produced with a cut-off in transverse momentum and, moreover, that the density matrix is such as to produce, in the decay, practically the maximum alignment along the incoming direction compatible with one unit of angular momentum, *i.e.* a $\cos^2\theta$ spectrum. We believe this connection between polarization effects of resonances and transverse-momentum cut-off to be quite general in the dual model. This should be the object of further theoretical investigations.

At the same time it would be invaluable if experimentalists could isolate resonance production in two-particle inclusive cross-sections from the probably large background of direct emission, and analyse whether their density matrix does exhibit strong polarization effects. The presence of such effects might sharply discriminate between various theoretical models for production.

2. – Method of computation.

Consider the loop amplitude represented in Fig. 2 *a*). It is useful to define

$$
\left\{
\begin{array}{lll}
p_1 = -p_6 = p_a\,, & p_2 = -p_5 = p_b\,, & p_3 = -p_4 = -p_c\,, \\
s = (p_1 + p_2)^2\,, & \bar{s} = (p_5 + p_c)^2\,, & \bar{s} = (p_5 + p_6)^2\,, \\
t = (p_2 + p_3)^2\,, & u = (p_1 + p_3)^2\,, & M^2 = (p_1 + p_2 + p_3)^2\,.
\end{array}
\right. \tag{2.1}
$$

The amplitude is then given by [5]

$$A(p_i) = g^6 \int \frac{\mathrm{d}^4 k}{(2\pi)^4} \int_0^1 \prod_{i=1}^{6} \mathrm{d}x_i x_i^{-\alpha(k_i^2)-1} I(x_i) \,, \tag{2.2}$$

where $\alpha(k^2) = \alpha_0 + \alpha' k^2$ is the linear Regge trajectory, k_i represents the momenta of the internal lines of the loop (we take as k_1 the momentum of the line between the external momenta p_6 and p_1; then $k_2 = k_1 + p_1$, etc.), k can be any of the momenta k_i, g^6 is the coupling constant which characterizes the dual expansion and

$$I(x_i) = \prod_{i=1}^{6} (1-x_i)^{\alpha_0-1} \prod_{n=1}^{\infty} (1-\omega^n)^{-4} \prod_{n=0}^{\infty} \prod_{i,j} (1-\omega^n x_{ij})^{-2\alpha' p_i \cdot p_j} \tag{2.3}$$

with

$$x_{ij} = x_{i+1} \dots x_j \,, \qquad \omega = x_{ii} = x_1 \dots x_6 \,.$$

The integrand appearing in eq. (2.2)

$$H(p_i, k_j) = \int_0^1 \prod_{i=1}^{6} \mathrm{d}x_i x_i^{-\alpha(k_i^2)-1} I(x_i) \tag{2.4}$$

develops poles whenever $\alpha(k_i^2) = n$. As a consequence $A(p_i)$ has branch points in M^2 corresponding to the normal thresholds in this variable. The discontinuity around these branch points is related to a contribution to the inclusive cross-section for the reaction a + b → c + anything:

$$2E_c \frac{\mathrm{d}\sigma^{\mathrm{loop}}}{\mathrm{d}\boldsymbol{p}_c} = \frac{1}{s} \lim_{\varepsilon \to 0} \frac{\mathrm{disc}_{M^2}}{2i} A(M^2, s + i\varepsilon, \bar{s} - i\varepsilon, t, u) \,. \tag{2.5}$$

To obtain the discontinuity around the normal thresholds, one must evaluate the residue of H at $\alpha(k_1^2) = n_1$, $\alpha(k_4^2) = n_4$, and sum

$$2E_c \frac{\mathrm{d}\sigma^{\mathrm{loop}}}{\mathrm{d}\boldsymbol{p}_c} = \frac{\pi^2}{s} g^6 \sum_{n_1, n_4} \int \frac{\mathrm{d}^4 k}{(2\pi)^4} \delta(\alpha(k_1^2) - n_1) \, \delta(\alpha(k_4^2) - n_4) \operatorname*{res}_{\substack{\alpha(k_1^2)=n_1 \\ \alpha(k_4^2)=n_4}} H(p_i, k_j) \,. \tag{2.6}$$

The factor

$$\operatorname*{res}_{\substack{\alpha(k_1^2)=n_1 \\ \alpha(k_4^2)=n_4}} H(p_i, k_j)$$

present in eq. (2.6) contains double poles of the form $1/(k_3^2 - m_R^2)(k_5^2 - m_R^2)$

corresponding to the propagators of the resonances R of Fig. 2 in the limit of zero width. As we said in the Introduction, we can conveniently describe the contribution to inclusive cross-sections from the production of the resonances R by replacing these double poles with a term $(\pi/\Gamma_R m_R)\delta(k_3^2 - m_R^2)$ (notice that $k_3 = k_5$ in the limit $\varepsilon = 0$).

The δ-function is obtained firstly by giving an imaginary part to the mass of the resonances in the propagators consistently to the fact that they are unstable particles, and then noticing that, if the width is small, the product of the two propagators can be approximated by a δ-function:

$$(2.7)\qquad \frac{1}{k_3^2 - m_R^2 + i\Gamma_R m_R}\,\frac{1}{k_5^2 - m_R^2 - i\Gamma_R^2 m_R^2} = (\text{for } k_3 = k_5) =$$

$$= \frac{1}{(k_3^2 - m_R^2)^2 + \Gamma_R^2 m_R^2} \simeq \frac{\pi}{\Gamma_R m_R}\,\delta(k_3^2 - m_R^2)\,.$$

(The opposite signs given to the widths depend on the fact that s and $\bar{s}$ must approach the real axis from different sides.)

Then every resonance R contributes to the inclusive cross-section by the following term:

$$(2.8)\qquad 2E_c\frac{\mathrm{d}\sigma_R}{\mathrm{d}\boldsymbol{p}_c} = \frac{\pi^2}{s}\,\frac{g^6}{\Gamma_R m_R}\sum_{n_1,n_4}\int\frac{\mathrm{d}^4k}{(2\pi)^4}\,\delta(\alpha(k_1^2) - n_1)\,\delta(\alpha(k_4^2) - n_4)\cdot$$

$$\cdot\,\delta(\alpha(k_3^2) - n)\operatorname*{res}_{\substack{\alpha(k_1^2)=n_1\ \alpha(k_4^2)=n_4\\ \alpha(k_3^2)=\alpha(k_5^2)=n}} H(p_i, k_j)\,.$$

The value of Γ_R can be computed in the dual model, and is of order g^2 for small coupling constant: thus we see that the effective contribution to the inclusive cross-section coming from the production of on-mass-shell resonances is of the same order of magnitude in g as those of the tree graphs (*)(**).

(*) It should be clear at this point that our method of computation requires that the resonances be narrow and that the interference between resonances separated in mass can be neglected (because we keep only diagonal terms in the sum over the resonances R). Therefore, as we said in the Introduction, it accounts for the production and decay of the first low-lying resonances of the spectrum, but will probably not be applicable to the region where resonances average out to a continuum.

(**) Our procedure of replacing the double poles in k_3^2 and k_5^2 with δ-functions divided by the width can be thought of also as a regularization of an infinity that would arise in the loop integration in eq. (2.6) when the values of the external momenta are such that the on-mass-shell condition for the resonances R can be met. Indeed, in the limit $\varepsilon = 0$, $k_3 = k_5$ and double poles of the form $1/(k_3^2 - m_5^2)^2$ are not integrable: a divergence in the integration over phase space arises. This divergence is not cured by the opposite $i\varepsilon$ prescription for s and $\bar{s}$, which in fact generates a pinch and a singularity for $\varepsilon \to 0$. Anyway, it is physically obvious that the integral over phase space should be divergent in eq. (2.6) because the resonances R appear there as stable particles of zero width.

The residue of $H(p_i, k_j)$, defined by eq. (2.4), in the multiple poles at $\alpha(k_1^2) = n_1$, $\alpha(k_4^2) = n_4$, $\alpha(k_3^2) = \alpha(k_5^2) = n$ can be evaluated by an expansion of $I(x)$ into powers of $x_1 x_3 x_4 x_5$. We used a computer program to perform the expansion at fixed values of the external momenta. The limitation on the size of the computation is given by the fact that the higher the numbers n_1, n_4 and n become, the more terms of the expansion must be evaluated. At the CERN computing facilities, values of the number N of necessary storage positions $\left(N = (n_1 + 1)(n_1 + n + 1)^2(n + 1)^2(n_1 + 1)\right)$ of the order of 8000 require only few seconds of processing per point of the spectrum. With such values of N we can compute spectra, for the first few resonances R, up to incoming centre-of-mass energies squared $s \approx 24(\alpha')^{-1}$.

The residue of H obtained from the expansion has the form of a finite sum of products of B-functions:

$$\text{(2.9)} \qquad \operatorname{res} H(p_i, k_j) = \sum_{n_2, n_6} c_{n_2, n_6}(p_i) B(-\alpha(s), -\alpha(k_2^2) + n_2) B(-\alpha(\bar{s}), -\alpha(k_6^2) + n_6).$$

The subsequent integration over k is a matter of kinematics: in the centre-of-mass frame of the incoming particles, for instance, it reduces to an integration over the angle φ between the plane α that contains the momenta $\boldsymbol{p}_a$, $\boldsymbol{p}_b$ and $\boldsymbol{p}_c$ and the plane β that contains $\boldsymbol{p}_c$, $\boldsymbol{p}_1$ and $\boldsymbol{p}_4$. Notice that the opening of the n_1, n_4 channels may result in a θ-function in the external kinematical variables; this explains the discontinuities in the spectra we shall display, discontinuities that would, of course, be smeared out by the finite widths of the resonances.

An important point about the computation is that the B-functions present in eq. (2.9) have poles whenever $\alpha(s)$ equals a nonnegative integer. To obtain a smooth cross-section in s (which is expected for large s) one cannot just take an average because of the presence of double poles of the form $1/(s - m_i^2)^2$, due to the zero-width resonances in the s-channel. There are two possibilities. One consists of assigning to these resonances a width Γ_i and taking the limit for $\Gamma_i \to 0$, thus replacing the double pole with $(\pi/\Gamma_i m_i)\delta(s - m_i^2)$. As discussed above, this procedure is probably correct when the interference between resonances of different masses is negligible. However, opposite to the case of the produced resonances, we are now interested in those values of the energy s for which the sum over resonances does build up a smooth continuum. Then one argues that it is appropriate to average (2.9) separately over $\alpha(s)$ and $\alpha(\bar{s})$ by means of the Stirling formula to produce a smooth function of s. This is the procedure we shall follow in Sect. **3**, but we will also display the results one would obtain from the first prescription.

Finally, we remark that almost all we have said is valid also for the amplitude associated to the twisted loop of Fig. 2 *b*); only slight modifications [6]

---

[6] V. ALESSANDRINI, D. AMATI, M. LE BELLAC and D. OLIVE: *Phys. Reports*, **1** C, 6 (1971); D. J. GROSS, A. NEVEU, J. SCHERK and J. H. SCHWARZ: *Phys. Rev. D*, **2**, 697 (1970).

are needed in eq. (2.3) and the residue of H takes the form

$$\text{(2.10)} \qquad \operatorname{res} H_r(p_i, k_j) = \sum_{n_2 n_6} c'_{n_2 n_6}(p_i) \cdot$$

$$\cdot B\big(-\alpha(k_2^2) + n_2, \alpha(s) + \alpha(k_2^2) + \alpha_0 - n_2\big) B\big(-\alpha(k_6^2) + n_6, \alpha(\bar{s}) + \alpha(k_6^2) + \alpha_0 - n_6\big) .$$

The B-functions appearing in eq. (2.10) have no poles in $\alpha(s)$ so that the smearing procedure we just discussed is not required.

3. – The inclusive spectra.

In this Section we report and discuss the results of the numerical computations of the inclusive spectra. The dual model, in its present form, is not appropriate for a description of the real hadron world, therefore only qualitative significance must be attached to our results (in particular, no attempt of data fitting can be made).

We recall that the consistency of the loop amplitude requires that all of the trajectories, both the internal ones and those on which the external particles lie, have the same intercept α_0. For most of the computations we fix $\alpha_0 = -0.16$, thus dealing with external particles of a common mass $\mu = 0.4(\alpha')^{-\frac{1}{2}}$ (*). We have chosen this value of μ to reduce kinematic effects, such as dips for zero transverse momentum of the detected particles. We will also exhibit, however, spectra computed for different values of μ.

In all the figures we display the quantity

$$\text{(3.1)} \qquad f(s, p_{c\perp}^2, x) = g^{-4} s E_c \frac{\mathrm{d}\sigma}{\mathrm{d}\boldsymbol{p}_c} ,$$

where $x = p_{cL}/|\boldsymbol{p}_a|$, and $p_{c\perp}$, p_{cL} stand for the transverse and longitudinal components of the momentum of the detected particle in the centre-of-mass frame. The scaling property, in terms of f, is defined by

$$\text{(3.2)} \qquad f(s, p_{c\perp}^2, x) = g(s) \hat{f}(p_{c\perp}^2, x) .$$

The function $g(s)$ will be given by s^{α_0} corresponding to pure Regge behaviour, but may have a different form in the presence of cuts.

Let us begin by showing in Fig. 4 *a*), 4 *b*) the spectra obtained from the tree graphs. We consider the tree graph of Fig. 1 *b*), with R = c. Figure 4 *a*) gives the spectrum in $p_{c\perp}^2$ for $x \simeq 0.75$ (**) (fragmentation region), Fig. 4 *b*) for

(*) α' fixes the scale of masses; in the following we shall set $\alpha' = 1$.

(**) The discontinuity of a tree graph contains a δ-function in $M^2 = (p_a + p_b - p_c)^2$. Therefore, the spectra in $p_{c\perp}^2$ involve different values of x in a range corresponding to fixed M^2.

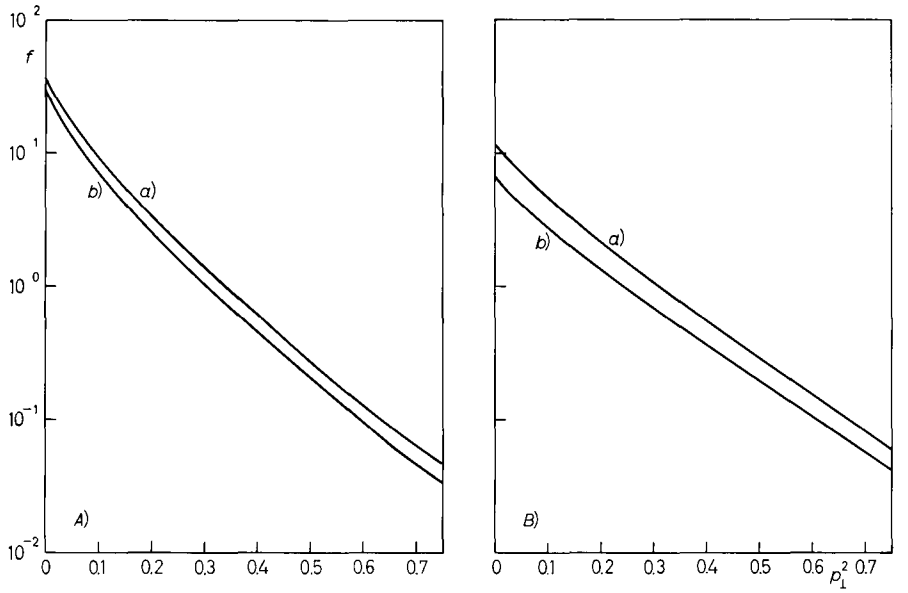

Fig. 4. – Spectra in $p_\perp^2$ computed from the tree diagrams of Fig. 1 *b*). Parameters: $\alpha_0 = -0.16$, $x = 0.75$ (Fig. 4 *a*)) and 0.05 (Fig. 4 *b*)), $\alpha(s) = 6$ (curves *a*)) and 12 (curves *b*)).

$x \simeq 0.05$ (pionization region) for $\alpha(s) = 6$ and 12. One should notice the presence of a cut-off in transverse momentum and a behaviour in s compatible with scaling (which is attained somewhat slower in the pionization region). The x-dependence of f for $\alpha(s) = 12$, $p_{c\perp}^2 = 0.1$ is reproduced in Fig. 5 (curve *a*).

We come to an analysis of the loop diagrams. There is a variety of loop diagrams that contain the phenomenon of resonance production. We consider in detail those of Fig. 2: Fig. 2 *a*) represents a typical planar loop, Fig. 2 *b*) exhibits a nonplanar one, which is often associated with the diffractive mechanism (7). We evaluate separately the contributions to the inclusive spectra that come from the different towers of resonances R. These towers characterized by $\alpha(k_3^2) = n$ contain degenerate resonances up to a maximum spin n. The contributions coming from the single resonances should be separately rescaled by the inverse of their widths (see eq. (2.8)). However, the fact that the number of resonances of the various towers is rapidly increasing with n makes it rather difficult, from a computational point of view, to separate the single contributions. Therefore, we shall confront with the tree graph the whole loop calculation evaluated with a common factor $g^2/m\Gamma$ which is the

(7) C. LOVELACE: *Phys. Lett.*, **34** B, 500 (1971); V. ALESSANDRINI, D. AMATI and B. MOREL: *Nuovo Cimento*, **7** A, 797 (1972); H. M. CHAN and P. HOYER: *Phys. Lett.*, **36** B, 79 (1971).

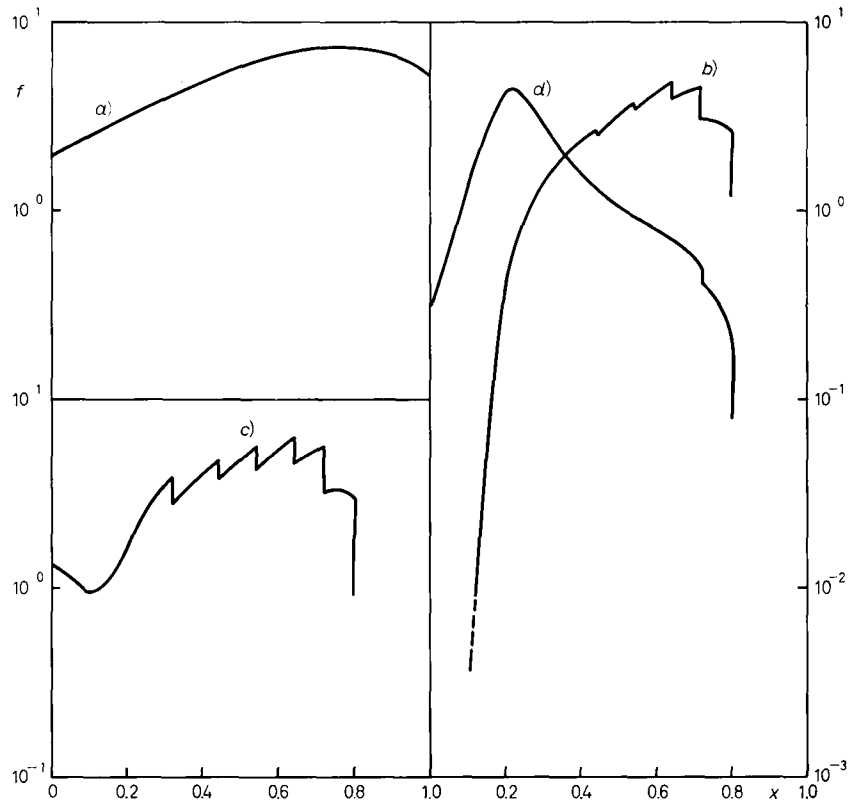

Fig. 5. – Spectra in x, computed from various diagrams (see text). Common parameters: $\alpha_0 = -0.16$, $\alpha(s) = 12$, $p_{c\perp}^2 = 0.1$.

appropriate one for the $J = 1$ resonance at $\alpha(k_3^2) = 1$. Thus we assign a common average width to the resonances of the various towers; we hope that this approximation does not distort too much the results to which, anyhow, we attach only qualitative significance (*).

With these considerations in mind, let us discuss the spectra reproduced in Fig. 5, 6, 7 and 8. The x-dependence of the contribution coming from the first tower of resonance ($\alpha = 1$, one resonance of spin 1 and one of spin 0) is given, for $p_{c\perp}^2 = 0.1$ and $\alpha(s) = 12$, in Fig. 5 (curves b and c) for the planar and nonplanar loops. The discontinuities are due to the opening up of intermediate channels. We see that the former is significant only in the fragmentation region of particle b, whereas the latter extends into the region of small x as well. This difference can be traced to the different mechanisms of production correspond-

(*) Having at our disposal a more realistic dual amplitude would justify the effort of rescaling and separating the various resonance contributions.

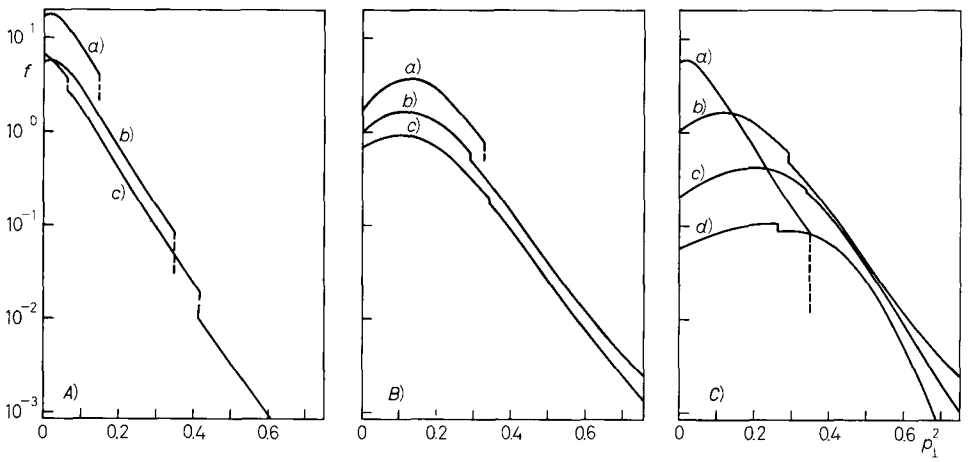

Fig. 6. – Spectra in $p_\perp^2$ from the diagram of Fig. 2 *a*) in the fragmentation region of b (see text for specification of parameters).

ing to Fig. 1 *a*) and 1 *b*). But interference effects between the produced resonances (of different spins, 1 and 0 in our case, and the same mass) are also important to explain the x distribution. Figure 5 (curve *d*) gives the analogous distribution obtained by twisting the R lines of the planar loop: since the resonances R are on the mass shell, the twist can only introduce a relative — sign between the contributions of the $J=1$ and $J=0$ components. We notice from Fig. 5 (curves *b* and *d*) that when we change the relative phase of these two contributions, the x behaviour of the result changes drastically.

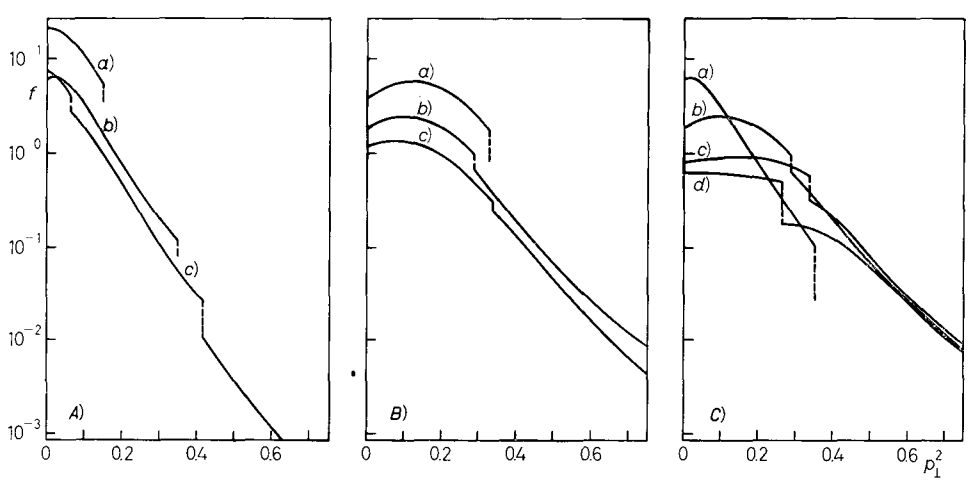

Fig. 7. – Spectra in $p_\perp^2$ from the diagram of Fig. 2 *b*) in the fragmentation region of b (see text for specification of parameters).

The assignment of different widths to the two resonances would not alter qualitatively the effect.

The dependence of the spectra on $p_{c\perp}^2$ is displayed in Fig. 6, 7, 8 and 9. Figure 6 *a*) gives the spectra obtained from the planar loop and the tower $\alpha(k_3^2) = 1$ for $x = 0.75$ and three different incoming energies ($\alpha(s) = 6, 12$ and 24 corresponding to curves *a*, *b* and *c*); Fig. 6 *b*) gives the spectra ob-

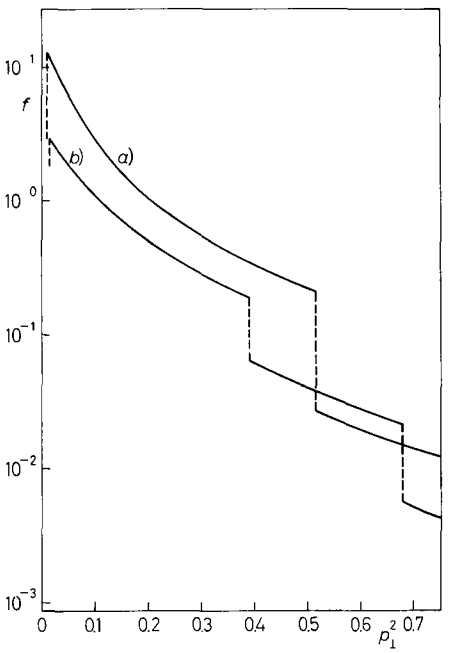

Fig. 8.

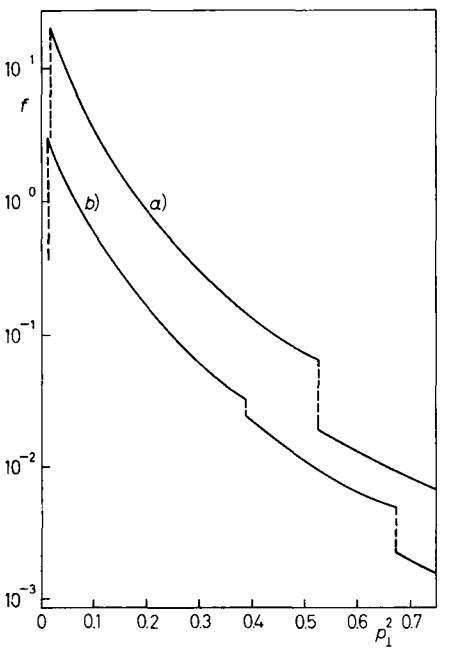

Fig. 9.

Fig. 8. – Spectra in $p_\perp^2$ from the diagram of Fig. 2 *b*) in central region (see text for specification of parameters).

Fig. 9. – Spectra in $p_\perp^2$ from the diagram of Fig. 2 *a*) with a twist on line R (see text for specification of parameters).

tained from the tower $\alpha(k_3^2) = 2$ for the same values of x and s. Figures 7 *a*) and 7 *b*) display the analogous spectra obtained from the nonplanar loop. We observe that a scaling regime is not reached at $\alpha(s) = 24$ (compare with the spectra obtained from the tree graph), but the smaller difference in the log scale between the curves for $\alpha(s) = 12$ and 24 with respect to the difference between $\alpha(s) = 6$ and 12 suggests that also the contribution from produced resonances may scale (*). The spectra for $\alpha(k_3^2) = 1, 2, 3$ and 4 (curves *a*,

(*) Scaling seems slower for the second tower than for the first.

b, *c* and *d*), $x = 0.75$ $\alpha(s) = 12$ are combined in Fig. 6 *c*) and 7 *c*). The spectra in $p_{c\perp}^2$ in the pionization region ($x = 0.05$) obtained from the non-planar loop for $\alpha(k_3^2) = 1$ and $\alpha(s) = 6$ and 12 (curves *a* and *b*) are given in Fig. 8; in Fig. 9 we see the analogous spectra obtained from the planar loop with a twist on the lines R.

From all of these spectra (Fig. 6 to 9) we see that a *cut-off in transverse momentum is preserved* (compare with the tree graph calculations of Fig. 4). We find this point very relevant and shall return to it in Sect. 4.

The numerical comparison of loop and tree contributions depends strongly on the rescale factor $g^2/m_R\Gamma_R$, but it appears that the loop is of the same order of magnitude of the tree, though somehow smaller.

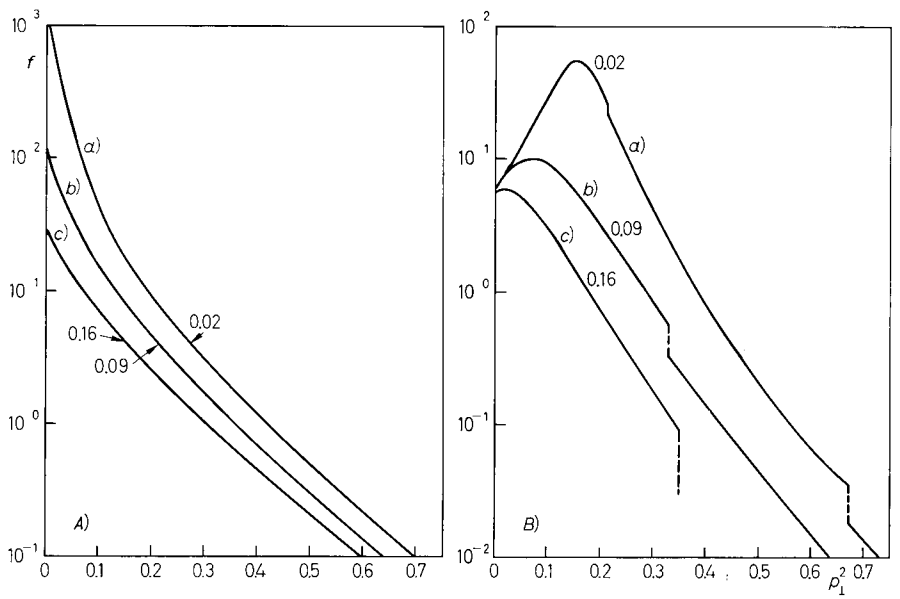

Fig. 10. – Dependence on spectra in $p_\perp^2$ on intercept parameter for diagrams of Fig. 1 *b*) and 2 *a*) (Fig. 10 *a*) and 10 *b*) respectively). Parameters: $\alpha(s) = 12$, $x = 0.75$, $\mu^2 = -\alpha_0$ indicated in the Figures.

Figure 10 exhibits the dependence of the spectra on the intercept parameter for the tree graph (Fig. 10 *a*)) and the planar loop (Fig. 10 *b*)). We observe that for small values of the external masses the loop contribution has a dip for small $p_{c\perp}^2$ which is due to kinematical effects.

Finally, in Fig. 11, we show the spectra obtained from a different prescription for averaging the singularities in *s*, *i.e.* replacing the double poles with $(\pi/m_i\Gamma_i)\delta(s - m_i^2)$. We display the spectra obtained according to this new rule, for the tree amplitude of Fig. 1 *a*) and the planar-loop amplitude. It seems that this alternative prescription, which should be correct for low *s*,

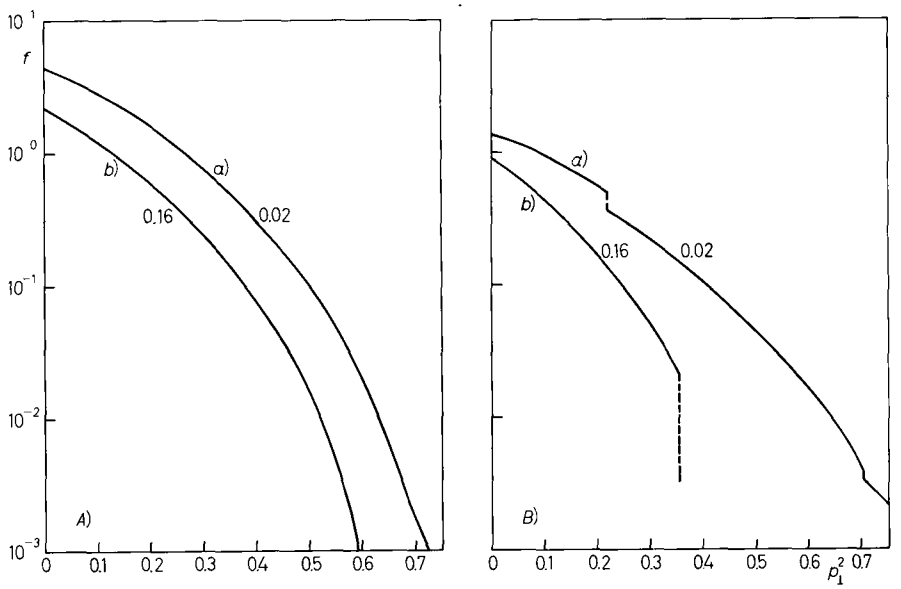

Fig. 11. – Spectra in $p_\perp^2$ obtained from a different averaging procedure on s-channel poles, for diagrams of Fig. 1 *a*) and 2 *a*) (Fig. 11 *a*) and 11 *b*) respectively). Parameters: $\alpha(s) = 12$, $x = 0.75$, $\mu^2 = -\alpha_0$ indicated in the Figures.

is not satisfactory regarding the features of the spectra at high energy. Essentially, it neglects the real parts of the amplitudes for the production of the intermediate state; this introduces a factor of $\sin^2 \pi\alpha(t)$ in the case of the tree amplitude and $\sin^2 \pi\alpha(k_2^2)$ for the loop amplitude, which distorts spectra particularly for small external masses. It is not mathematically clear how the transition between low- and high-energy regions occurs, however it appears that the prescription used for all our spectra, except for those of Fig. 11, which takes into account the real part of the amplitude for resonance production is the most appropriate for considering high-energy inclusive features.

4. – Some features of resonance production.

The cut-off in transverse momentum present in the contribution to inclusive cross-sections that come from resonance production suggests that

i) the resonances themselves are produced with a cut-off in transverse momentum;

ii) perhaps a mechanism is operating by which the resonances are produced with a strong polarization, which favours low values of $p_\perp^2$ for their decay products.

In this Section we investigate these two points (*). We factor out of the loop amplitude (for definiteness we consider the planar loop of Fig. 2 *a*)) the tree amplitude $A_{\mu\nu}$ for the forward scattering of two ground state scalars of momenta p_a and p_b, with an excited state of the first level of spin 1 and momentum p. $A_{\mu\nu}(p_a, p_b, p)$ is given by

$$A_{\mu\nu} = B_1 p_{a\mu} p_{a\nu} + B_2 p_{b\mu} p_{b\nu} + B_3(p_{a\mu} p_{b\nu} + p_{b\mu} p_{a\nu}) + B_4 g_{\mu\nu}, \tag{4.1}$$

where the scalar amplitudes $B_i(p_a, p_b, p)$ are given by

$$\left\{\begin{aligned} B_1 &= \int \mathrm{d}x_1 \mathrm{d}x_2 \mathrm{d}x_3 x_1 x_3 (1 - x_2^2) I(x_i, p_j), \\ B_2 &= \int \mathrm{d}x_1 \mathrm{d}x_2 \mathrm{d}x_3 (1 - x_1 x_2 x_3)^2 I(x_i, p_j), \\ B_3 &= \int \mathrm{d}x_1 \mathrm{d}x_2 \mathrm{d}x_3 \left(\frac{x_1 + x_3}{2}\right)(1 - x_2)(1 - x_1 x_2 x_3) I(x_i, p_j), \\ B_4 &= \int \mathrm{d}x_1 \mathrm{d}x_2 \mathrm{d}x_3 (x_1 x_2 x_3) I(x_i, p_j), \end{aligned}\right. \tag{4.2}$$

and $I(x_1, x_2, x_3, p_a, p_b, p)$ is the integrand that appears in the formula for the analogous tree amplitude involving only ground state particles.

The inclusive cross-section for the production of the resonance is related to the discontinuity of $A_{\mu\nu}$ in the variable $M^2 = (p_a + p_b - p)^2$ according to the equation

$$2E_c \frac{\mathrm{d}\sigma_R}{\mathrm{d}\boldsymbol{p}_c} = \frac{1}{s} \sum_i \varepsilon_\mu^{(i)*} \left(\frac{\mathrm{disc}_{M^2}}{2i} A^{\mu\nu}\right) \varepsilon_\nu^{(i)}, \tag{4.3}$$

where $\varepsilon_\mu^{(i)}$ denotes the polarization vectors of the resonance.

The density matrix is given by

$$\varrho_{i,j} = \frac{\varepsilon_\mu^{(i)*} \left(\frac{\mathrm{disc}_{M^2}}{2i} A^{\mu\nu}\right) \varepsilon_\nu^{(j)}}{\sum_i \varepsilon_\mu^{(i)*} \left(\frac{\mathrm{disc}_{M^2}}{2i} A^{\mu\nu}\right) \varepsilon_\nu^{(i)}}. \tag{4.4}$$

The dependence of $2E_c(\mathrm{d}\sigma_R/\mathrm{d}\boldsymbol{p}_c)$ on the transverse component of p is exhibited in Fig. 12, where we plot the quantity $f_R(s, p_\perp^2, x) = sE_c(\mathrm{d}\sigma_R/\mathrm{d}\boldsymbol{p}_c)$ evaluated

(*) For an analysis of resonance production in the dual resonance model, see also DI GIACOMO and KONISHI (8).

(8) A. DI GIACOMO and K. I. KONISHI: M.I.T. preprint 278 (1972).

numerically for $\alpha(s) = 12$, $x = (p_L/|p_a|) \approx 0.75$ and two different values ($\alpha_0 = -0.02$ and $\alpha_0 = -0.09$) of the intercept parameter.

Notice that a cut-off in transverse momentum is in fact present, and that, after a sharper peak for small $p_\perp^2$, the behaviour of the spectrum is essentially exponential in $p_\perp^2$.

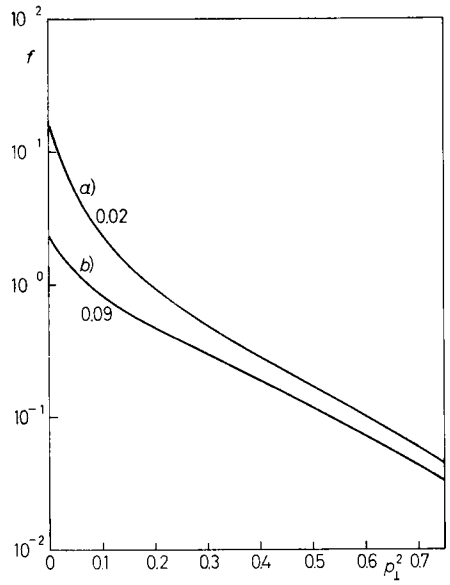

Fig. 12. – Spectra in $p_\perp^2$ for inclusive resonance production. Parameters: $\alpha(s) = 12$, $x = 0.75$, $\mu^2 = -\alpha_0$ indicated in the Figures.

The polarization of the produced resonance can be deduced from the density matrix, or, equivalently, by considering the bilinear form

$$A(\boldsymbol{q}) = \sum_{ij} q_i \left(\frac{\mathrm{disc}_{M^2}}{2i} A_{ij} \right) q_j , \tag{4.5}$$

where A_{ij} is the space part of $A_{\mu\nu}$ in the rest frame of the resonance.

$A(\boldsymbol{q})$ measures the probability that the relative momentum of the decay products of the resonance in its rest frame is given by $\boldsymbol{q}$. By a rotation of the frame of reference, $A(\boldsymbol{q})$ can be reduced to the diagonal form

$$A(\boldsymbol{q}) = \sum_i \alpha_i (q_i')^2 . \tag{4.6}$$

Then $\alpha_1 = \alpha_2 = \alpha_3$ imply an isotropic decay in the rest frame of the resonance, whereas maximum polarization is obtained when two of the α_i are zero.

From numerical computations done for a wide range of parameters s, $x = p_L/|p_a|$, $p_\perp^2$ and α_0 we have found that the decay is always almost maximally anisotropic, *i.e.* that one of the α's always dominates the other two. What happens is that the function B_2 of eq. (4.1) turns out to be of some orders of magnitude larger than B_1 and B_4, B_3 being consistent with an almost factorized expression

$$A_{\mu\nu} = (b_1 p_{b\mu} + b_2 p_{a\mu})(b_1 p_{b\nu} + b_2 p_{a\nu}) , \tag{4.7}$$

where $b_1 \gg b_2$.

Then, in its rest frame, the resonance decays preferentially in the direction of the incoming particle b, with an almost pure $\cos^2\theta$-dependence which is the maximum alignment compatible with spin 1 (*).

Thus we see that the cut-off in the transverse momentum of the final stable particle is reproduced, in the dual-resonance model, both through a cut-off in the transverse momentum of the produced resonance and strong polarization effects. These polarization effects seem to be a very relevant feature of the model itself. Of course, we have established them only in a rather limited example, and cannot claim that they are of all generality.

It would be an interesting theoretical task to find out whether a strong polarization of produced spinning particles is in fact a quite general prediction of the dual resonance model.

At the same time it would be extremely important to see whether these polarization effects are supported by experimental data. It may be rather difficult to separate the production of a resonance in a two-body inclusive reaction from the presumably large background of primary produced particles. But a detailed experimental analysis of the inclusive production of a resonance and, in particular, of its polarization could contribute some fundamental information to our understanding of high-energy processes and help to discriminate among the various theoretical models that are proposed to explain them.

* * *

We wish to thank A. DELLA SELVA for contributions in the early stage of this work, V. ALESSANDRINI and G. VENEZIANO for useful discussions, D. AMATI for useful discussions and a careful reading of the manuscript. One of us (L.M.) wishes to thank the Theoretical Study Division of CERN for the hospitality extended to him.

(*) Analogous results for the polarization of a particle of spin one within the dual resonance model have been obtained by FENSTER and URETSKY [9], who consider a different kinematical region (the central region) and employ asymptotic techniques; they also find almost maximal anisotropy in the decay.

[9] S. FENSTER and J. L. URETSKY: ANL/HEP 7212 (1972).

● RIASSUNTO (*)

Si calcola numericamente il contributo delle risonanze intermedie prodotte agli spettri inclusivi tramite la discontinuità delle ampiezze duali ad un'ansa. Si trova che questi contributi sono minori ma non trascurabili rispetto a quelle provenienti dai grafici ad ansa che per quelli ad albero. Si mantiene il taglio nell'impulso trasversale anche per una risonanza intermedia prodotta piuttosto pesante. Si argomenta che questo fatto è in relazione con i forti effetti di polarizzazione nel decadimento di risonanze nel modello duale.

(*) *Traduzione a cura della Redazione.*

Рождение резонансов и включающие поперечные сечения в дуальных моделях.

Резюме (*). — Мы численно рассчитываем вклад промежуточных резонансов в включающие спектры, используя разрыв дуальных амплитуд с одной петлей. Мы получаем, что эти вклады оказываются меньше, но не пренебрежимо малыми, по сравнению с вкладами от древовидных графиков. Подобие может быть достигнуто для петельных диаграмм при более высоких энергиях, чем для древовидных. Обрезание поперечного импульса сохраняется даже для довольно тяжелых промежуточных резонансов. Мы показываем, что этот факт связан с сильными поляризационными эффектами при распаде резонансов в дуальной модели.

(*) *Переведено редакцией.*

CERN
SERVICE D'INFORMATION
SCIENTIFIQUE

L. MASPERI, *et al.*
1 Febbraio 1973
Il Nuovo Cimento
Serie 11, Vol. **13** A, pag. 689-707